

# Time-Resolved Detection of Structural Changes During the Photocycle of Spin-Labeled Bacteriorhodopsin

Heinz-Jürgen Steinhoff, Ramin Mollaaghababa, Christian Altenbach, Kálmán Hideg, Mark Krebs, H. Gobind Khorana,\* Wayne L. Hubbell\*

Bacteriorhodopsin was selectively spin labeled at residues 72, 101, or 105 after replacement of the native amino acids by cysteine. Only the electron paramagnetic resonance spectrum of the label at 101 was time-dependent during the photocycle. The spectral change rose with the decay of the M intermediate and fell with recovery of the ground state. The transient signal is interpreted as the result of movement in the C-D or E-F interhelical loop, or in both, coincident with protonation changes at the key aspartate 96 residue. These results link the optically characterized intermediates with localized conformational changes in bacteriorhodopsin during the photocycle.

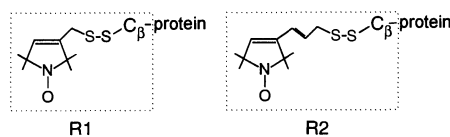
Bacteriorhodopsin (bR) serves as a light-driven proton pump in the purple membrane of *Halobacterium salinarium* (1). Photon absorption by the intrinsic all-trans retinal chromophore initiates a cyclic series of transformations between discrete intermediates identified by their optical absorbance maxima and kinetic properties (2). During this photocycle, a proton is translocated across the membrane (Fig. 1).

Bacteriorhodopsin offers a unique opportunity to study molecular mechanisms of an active transport system because a structural model of the bR ground state is available (3) and site-specific mutagenesis enables the preparation of a variety of bR mutants in a form similar to that of the wild-type protein lattice (4). The intermediates observed in the bR photocycle reflect conformational changes in the membrane protein. Both neutron and electron diffraction studies on bR cold-trapped during the photocycle have revealed changes in the projected structure (5). Time-resolved x-ray diffraction studies on mutants with a slow photocycle have detected similar changes (6). In addition, time-resolved Fourier transform infrared (FTIR) spectroscopy has identified structural changes in the protein backbone during the M to N transition (7). However, none of the above approaches have provided both real-time resolution and localization of the structural changes.

Site-directed spin labeling (SDSL) offers a promising approach to localize structural

changes with a time resolution sufficient to observe the intermediates in the latter half of the photocycle. Here we report the time-resolved detection of a reversible structural change in bR during the photocycle using SDSL and show that it is associated with a state lying between the M intermediate and bR ground state.

The development of site-directed mutagenesis has made it possible to obtain specific attachment sites for spin labels in a protein with the use of cysteine substitution mutants (8). We have used bR mutants V101C, Q105C, and G72C (9) expressed in *H. salinarium* and purified in a two-dimensional lattice form similar to that of wild-type bR (10). These mutants were modified at the single reactive sulfhydryl group with either (1-oxyl-2,2,5,5-tetramethylpyrroline-3-methyl)methanethiosulfonate or (1-oxyl-2,2,5,5-tetramethylpyrroline-3-trans-propene)methanethiosulfonate to give nitroxide side chains designated R1 or R2, respectively (11).



The shapes of the electron paramagnetic resonance (EPR) spectra of the mutants in the lattice (Fig. 2, a through d) reflect the internal motion of the nitroxide side chains, which is in turn determined by the degree of interaction with nearby groups in the protein. The spectra of C101R1 and C72R1 (12) (Fig. 2, a and c) reflect intermediate immobilization of the nitroxides and are similar to those reported earlier for monomeric bR (13, 14). This suggests that the interactions restricting the motions are intramolecular and not between the nitroxides and adjacent bR molecules in the lattice. However, the EPR spectrum for C105R1 reflects strong immobilization of

the nitroxide (Fig. 2d), in contrast to the high degree of mobility observed in the monomeric state (13). Thus, the immobilization in the lattice must be the result of intermolecular interactions. The nitroxide in the side chain of C101R2 is extended from the backbone by about 3 Å relative to that in C101R1, resulting in an increase of the label mobility (compare Fig. 2, a and b).

These results can be compared with the bR structural model shown in Fig. 3. The nitroxide in C101R1 interacts with groups in the E-F interhelical loop, consistent with the partial intramolecular immobilization noted above. The nitroxide side chain at C105R1 points outward with limited intramolecular contacts, consistent with the high mobility of the label in monomeric bR (13). However, in the lattice, this side chain would make direct contact with the B helix of a neighboring bR molecule (3, 5), resulting in the strong immobilization observed. Reliable conclusions regarding the interactions of a nitroxide at C72R1 cannot be drawn because of the uncertainty in the conformation of the relatively long B-C loop. The increased nitroxide mobility in C101R2 relative to C101R1 can be understood in terms of the model because an increase in the length of the side chain moves the nitroxide group away from interaction with the tip of the E-F interhelical loop.

Changes in the EPR spectra caused by photoexcitation were monitored directly during a magnetic field scan by phase-sensitive detection referenced to the triggering source of a xenon flash lamp (150- $\mu$ s duration, 0.5-Hz repetition rate). This detection scheme gives directly the difference EPR spectrum between excited and ground-state conformations. A difference spectrum is observed for C101R1 during the photocycle (Fig. 2e). This is unambiguously interpreted as a decrease in nitroxide mobility as judged by the changes in amplitude at the spectral extremes. The conformational change of the protein causing this change is not likely

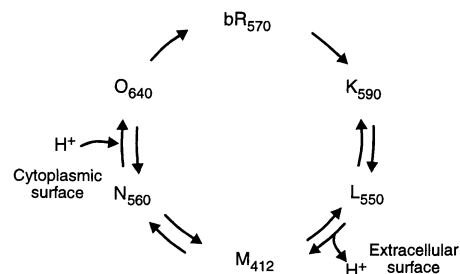


**Fig. 1.** The photocycle of bR. The scheme is that of Lozier *et al.* (2), with the addition of back reactions. Although a single intermediate is shown for M, it has been proposed that there are at least two distinct forms. The wavelengths of maximal absorbance are given for each intermediate.

H.-J. Steinhoff, Institut für Biophysik, Ruhr-Universität Bochum, 44780 Bochum, Germany.

R. Mollaaghababa, M. Krebs, H. G. Khorana, Departments of Biology and Chemistry, Massachusetts Institute of Technology, Cambridge, MA 02139, USA.

C. Altenbach and W. L. Hubbell, Jules Stein Eye Institute and Department of Chemistry and Biochemistry, University of California, Los Angeles, CA 90024-7008, USA.

K. Hideg, Central Research Laboratory, Chemistry, University of Pécs, H-7643 Pécs, Hungary.

\*To whom correspondence should be addressed.

to be global because no difference spectra were detected for C72R1 or C105R1 (Fig. 2, g and h). Mutant C101R2 has a difference spectrum of lower amplitude but of the same character (Fig. 2, f). This is expected because R2 at this site has weaker tertiary interactions and is less sensitive to changes in structure.

To correlate the light-induced spectral change with a specific intermediate of the photocycle, we recorded the time dependence of the EPR signal following a light flash with the magnetic field fixed at the maximum of the difference signal (Fig. 4). For both C101R1 and C101R2, the EPR spectral changes appear with the decay of  $M_{412}$  and reverse with the recovery of the  $bR_{570}$  ground state. Therefore, structural changes take place during the formation of the N or O intermediates, or both (Fig. 1). These results are consistent with those from time-resolved FTIR experiments (7).

The photocycles of V101C, Q105C, and G72C are similar to the wild-type protein (15). However, the photocycles of spin-labeled derivatives C101R1 and C101R2 are slowed by factors of 10 and 2, respectively (Fig. 4), whereas those of C105R1 and C72R1 are the same as wild type. The effects of the spin labels on the photocycle are mirrored in the magnitude of the EPR signal change (compare Fig. 2, e through h). This is not unexpected because structural changes are detected through interaction of the spin label with the protein. If the protein structural transition is coupled to an optical transient, such interaction must

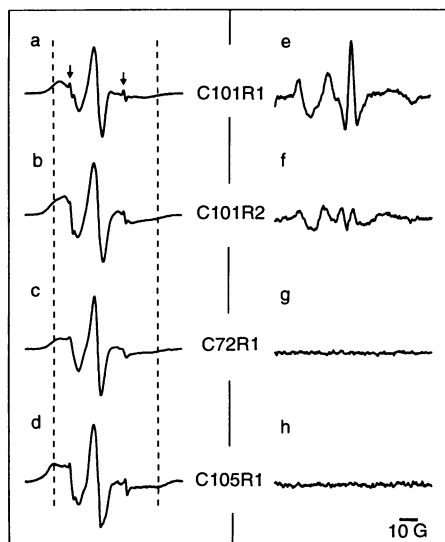


**Fig. 2.** Ground-state EPR spectra (a through d) and difference spectra detected during the photocycle (e through h) for the indicated species. The dotted vertical lines indicate the positions of the outer hyperfine extrema that characterize immobilized nitroxides. The arrows in (a) indicate the signal from a small amount (<1%) of unreacted spin label that is present in each sample (a through d).

necessarily modify the kinetics of the photocycle in a manner related to the strength of the interaction.

What kind of structural perturbation could give rise to the change in the EPR spectra? The nitroxide in C101R1 is predicted to be in contact with the E-F interhelical loop (Fig. 3), and appropriate movements of helices E, F, C, or D at the cytoplasmic surface could alter the nitroxide mobility. The spin label in C105R1 does not sense any changes upon photoexcitation, suggesting that the cytoplasmic part of helix D does not move. Because C105R1 contacts the B helix of an adjacent bR molecule in the protein lattice trimer, the absence of a spectral change also implies a lack of movement at the cytoplasmic end of helix B. Therefore, we conclude that the transient spectral change is the result of movement in the E-F or C-D interhelical loop, or in both. Finally, the lack of change detected by C72R1 suggests that residues at the extracellular surface of bR associated

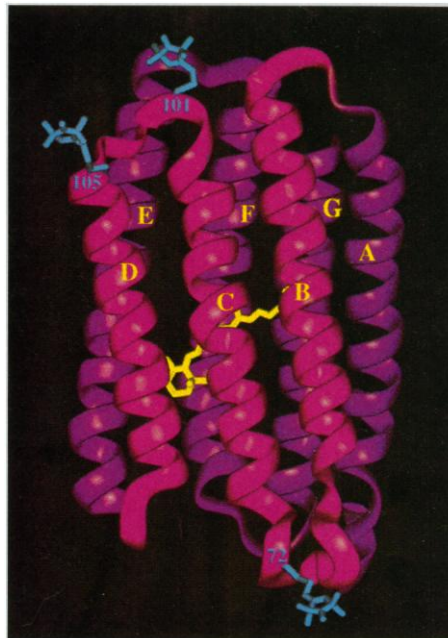


**Fig. 3.** The structure of the bR backbone. The helices are identified as A-G, and the side chain R1 at 72, 101, and 105 is shown as a stick model. Coordinates of the helical segments were obtained from the Brookhaven Protein Data Bank. Helix D was shifted by 3 Å toward the cytoplasmic side, as suggested by recent diffraction data (19). Coordinates for the interhelical loops and nitroxide side chains were constructed by homology and energy minimization methods (20). The C-D interhelical loop (residues 101 to 105) is very short, with a narrow range of conformations available. For all energetically reasonable conformations, the primary interactions of a spin label at 101 is with the E-F loop, while spin labels at 105 point outward from the molecule, as shown. The B-C interhelical loop containing residue 72 is relatively long (residues 63 to 73), and the predicted conformation less certain.

with B or C do not undergo significant rearrangement during the latter half of the photocycle.

A comparison of the EPR results with those obtained from diffraction experiments (5, 6) reveals an important difference. The EPR data indicate that the conformations of M and the ground state are similar in the region of the nitroxides. On the other hand, electron density difference projection maps show large changes at M, which relax upon return to the ground state. This difference may be due to the fact that projection electron density maps reflect all changes along the length of the molecule, whereas SDSL detects only changes near the nitroxide and in this sense has a higher spatial resolution. Thus, the structural perturbations assigned to the M intermediate in diffraction experiments either occur at sites distant from 101 or are caused by the presence of intermediates beyond M in the samples.

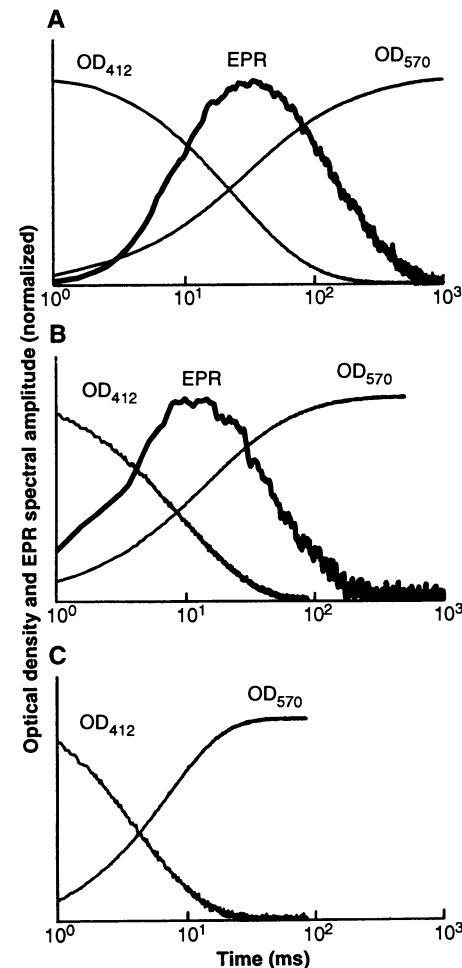


**Fig. 4.** Normalized optical densities (ODs) and EPR spectral amplitudes recorded as a function of time following a light flash for mutant (A) C101R1 and (B) C101R2. Optical densities at 412 nm and 570 nm monitor the M intermediate and ground state, respectively. For comparison, (C) the optical density transients for the wild-type protein are shown.

Recently, reversible light-induced conformational changes were observed with the use of a spin label in the C-D interhelical loop in rhodopsin (16). It is significant that the changes in bR structure are also detected by a label in the C-D interhelical loop. Furthermore, the changes in both proteins evidently coincide with protonation changes at the Schiff base linkage of the retinal chromophore.

As for the functional significance of the structural changes in bR, Asp<sup>96</sup>, five residues from the spin label at 101, is protonated in the ground state, transfers a proton to the Schiff base during M decay, and is reprotonated from solution during the decay of N (Fig. 1) (17). Evidently, the EPR signal changes are coincident with this process and thus may reflect structural changes near 101 as a result of changes in the protonation of Asp<sup>96</sup>. An interesting possibility is that the transient change reflects the opening and closing of a pathway from the aqueous solution to Asp<sup>96</sup> (3, 7). Recently, a change in local electrostatic potential around residue 101 was reported to have a similar relative time course (18).

In conclusion, a conformational change occurs during the decay of the M intermediate and reverses during the return to the ground state. The change is localized to the cytoplasmic side of the protein, in the vicinity of the E-F and C-D interhelical loops, and may reflect protonation changes in Asp<sup>96</sup>. In principle, all of the conformational changes during the photocycle can be mapped by SDSL with a sufficiently large set of spin-labeled mutants.

REFERENCES AND NOTES

1. W. Stoeckenius, R. H. Lozier, R. A. Bogomolni, *Biochim. Biophys. Acta* **505**, 215 (1978); H. G. Khorana, *J. Biol. Chem.* **263**, 7439 (1988); D. Oesterhelt, C. Bauchle, N. Hampp, *Q. Rev. Biophys.* **24**, 425 (1991).
2. R. H. Lozier, R. A. Bogomolni, W. Stoeckenius, *Biophys. J.* **15**, 955 (1975).
3. R. Henderson et al., *J. Mol. Biol.* **213**, 899 (1990).
4. M. P. Krebs and H. G. Khorana, *J. Bacteriol.* **175**, 1555 (1993).
5. N. A. Dencher, D. Dresselhaus, G. Zaccai, G. Büldt, *Proc. Natl. Acad. Sci. U.S.A.* **86**, 7876 (1989); S. Subramaniam, M. Gerstein, D. Oesterhelt, R. Henderson, *EMBO J.* **12**, 1 (1993).
6. M. H. Koch et al., *EMBO J.* **10**, 521 (1991).
7. G. Souvignier and K. Gerwert, *Biophys. J.* **63**, 1393 (1992); K. J. Rothschild et al., *J. Biol. Chem.* **268**, 27046 (1993).
8. A. P. Todd, J. Cong, F. Levinthal, C. Levinthal, W. L. Hubbell, *Proteins* **6**, 294 (1989); C. Altenbach, T. Marti, H. G. Khorana, W. L. Hubbell, *Science* **248**, 1088 (1990).
9. To designate mutants, we give the single-letter code for the original amino acid, then the position of the amino acid, and finally the single-letter code for the replacement. Single-letter codes: C, Cys; G, Gly; Q, Gln; and V, Val.
10. Mutant plasmids were constructed by replacement of the Asp 718-Bsp HI fragment of the native *bop* gene with a synthetic piece carrying the appropriate mutation. Expression and purification of the mutant proteins were carried out as described previously for

- other mutants [M. P. Krebs, R. Mollaaghababa, H. G. Khorana, *Proc. Natl. Acad. Sci. U.S.A.* **90**, 1987 (1993)].
11. Spin labeling was carried out in the presence of a fivefold molar excess of the label for 12 hours at 22°C. Excess label was removed by centrifugal washing. The stoichiometry in each case was 0.7 to 0.8 labels per bR. Spectra were recorded at 25°C at X-band frequencies in a TM101 cavity.
12. To designate mutants with spin-labeled side chains R1 or R2, we use the notation CXR1 or CXR2, where C is the original cysteine and X is the position of the amino acid.
13. D. A. Greenhalgh, C. Altenbach, W. L. Hubbell, H. G. Khorana, *Proc. Natl. Acad. Sci. U.S.A.* **88**, 8626 (1991).
14. C. Altenbach, S. L. Flitsch, H. G. Khorana, W. L. Hubbell, *Biochemistry* **28**, 7806 (1989).
15. U. Alexiev, R. Mollaaghababa, H. G. Khorana, M. P.

- Heyn, unpublished data.
16. J. F. Resek, Z. T. Farahbakhsh, W. L. Hubbell, H. G. Khorana, *Biochemistry* **32**, 12025 (1993); Z. T. Farahbakhsh, K. Hideg, W. L. Hubbell, *Science* **262**, 1416 (1993).
17. K. Gerwert, G. Souvignier, B. Hess, *Proc. Natl. Acad. Sci.* **87**, 9774 (1990).
18. U. Alexiev, T. Marti, M. P. Heyn, H. G. Khorana, P. Scherrer, *Biophys. J.* **66**, A44 (1994).
19. R. Henderson, personal communication.
20. Insight II, Homology, and Discover; Biosym Technologies, San Diego, CA.
21. Supported by a Max Kade Foundation Fellowship (H.-J.S.); NIH grants GM28289 (H.G.K.) and EY05216 (W.L.H.); Hungarian Research Foundation grant OTKA/3/42 (K.H.); and the Jules Stein Professor endowment (W.L.H.).

21 June 1994; accepted 2 August 1994

## Cystic Fibrosis Heterozygote Resistance to Cholera Toxin in the Cystic Fibrosis Mouse Model

Sherif E. Gabriel,\* Kristen N. Brigman, Beverly H. Koller, Richard C. Boucher, M. Jackson Stutts

The effect of the number of cystic fibrosis (CF) alleles on cholera toxin (CT)-induced intestinal secretion was examined in the CF mouse model. CF mice that expressed no CF transmembrane conductance regulator (CFTR) protein did not secrete fluid in response to CT. Heterozygotes expressed 50 percent of the normal amount of CFTR protein in the intestinal epithelium and secreted 50 percent of the normal fluid and chloride ion in response to CT. This correlation between CFTR protein and CT-induced chloride ion and fluid secretion suggests that CF heterozygotes might possess a selective advantage of resistance to cholera.

Cystic fibrosis (CF) is the most common, fatal, homozygous recessive disorder of the Caucasian population. One in 20 Caucasians harbors one copy of the mutated CF gene, resulting in a frequency of CF of 1 in every 2500 live births. CF is characterized by decreased Cl<sup>-</sup> permeability of the apical membrane of many epithelial tissues (1), a result of mutations in the CF gene (2), and can result in meconium ileus in CF newborns and intestinal obstructions and accumulation of mucus in older individuals with CF (3). Secretory diarrhea may be caused by colonization of the small intestine with the organism *Vibrio cholerae* and results in a voluminous Cl<sup>-</sup> and fluid secretion that can be fatal if untreated (4). Cholera mediates its action by an irreversible elevation of the concentration of intracellular adenosine 3',5'-monophosphate (cAMP), which triggers sustained Cl<sup>-</sup> and fluid secretion (4, 5). These two diseases are connected by the apically located, cAMP-regulated, Cl<sup>-</sup> channel CFTR. It has been proposed that CF heterozygotes may have a selective advantage against cholera-induced secretory diarrhea (6). The hypothesis suggests that

CFTR Cl<sup>-</sup> conductance is the rate-limiting step for intestinal Cl<sup>-</sup> and fluid secretion, and therefore the hypothesis predicts a direct relation between CFTR expression and resultant Cl<sup>-</sup> secretion.

Efforts to test this hypothesis have been limited by the absence of an animal model for CF (7). The CFTR(-/-) mouse was created by disruption of the CF gene at exon 10 by insertion of an in-frame stop codon (designated X) to replace Ser<sup>489</sup> (S489X). This stop codon results in an unstable, truncated CFTR message and no full-length CFTR protein (8). Heterozygotes carrying one copy of the normal CFTR gene and one copy of the disrupted gene were crossed to give offspring that express zero, one, or two normal CFTR alleles and were designated CFTR(-/-) (homozygote CF), CFTR(+/-) (heterozygote), or CFTR(+/+) (homozygote normal), respectively. Heterozygote CFTR(+/-) mice were bred to C57BL/6 mice for at least six generations, with selection at each generation for the presence of the S489X mutation. After six generations, when over 98% of the loci were expected to be identical to C57BL/6, these heterozygous animals were mated with one another, and CFTR(+/-), CFTR(+/-), and CFTR(-/-) mice were obtained. These breeding strategies provided an opportunity to

Department of Medicine, University of North Carolina, Chapel Hill, NC 27599, USA.

\*To whom correspondence should be addressed.